Technical Note

Quantification of Epithelial Cells in Coculture With Fibroblasts by Fluorescence Image Analysis

Ana Krtolica,[1] Carlos Ortiz de Solorzano,[1] Stephen Lockett,[2] and Judith Campisi[1]*

[1]Life Sciences Division, Lawrence Berkeley National Laboratory, Berkeley, California
[2]National Cancer Institute, Frederick, Maryland

Received 28 January 2002; Revision Received 10 July 2002; Accepted 18 July 2002

Background: To demonstrate that senescent fibroblasts stimulate the proliferation and neoplastic transformation of premalignant epithelial cells (Krtolica et al.: Proc Natl Acad Sci USA 98:12072–12077, 2001), we developed methods to quantify the proliferation of epithelial cells cocultured with fibroblasts.

Methods: We stained epithelial–fibroblast cocultures with the fluorescent DNA-intercalating dye 4,6-diamidino-2-phenylindole (DAPI), or expressed green fluorescent protein (GFP) in the epithelial cells, and then cultured them with fibroblasts. The cocultures were photographed under an inverted microscope with appropriate filters, and the fluorescent images were captured with a digital camera. We modified an image analysis program to selectively recognize the smaller, more intensely fluorescent epithelial cell nuclei in DAPI-stained cultures and used the program to quantify areas with DAPI fluorescence generated by epithelial nuclei or GFP fluorescence generated by epithelial cells in each field.

Results: Analysis of the image areas with DAPI and GFP fluorescences produced nearly identical quantification of epithelial cells in coculture with fibroblasts. We confirmed these results by manual counting. In addition, GFP labeling permitted kinetic studies of the same coculture over multiple time points.

Conclusions: The image analysis–based quantification method we describe here is an easy and reliable way to monitor cells in coculture and should be useful for a variety of cell biological studies. Cytometry 49:73–82, 2002. © 2002 Wiley-Liss, Inc.

Key terms: cell quantification; coculture; image analysis; epithelial–stromal interactions; cell proliferation; green fluorescent protein; 4,6-diamidino-2-phenylindole; fluorescence microscopy

Cell–cell interactions in general and epithelial–stromal cell interactions in particular are essential components of the cellular microenvironment. The cellular microenvironment is important for many basic cellular processes such as proliferation and differentiation and pathological processes such as tumorigenesis (1–7). Among the crucial signals that govern cell behavior are those generated locally by neighboring cells. To study these signaling mechanisms in a controlled setting, several coculture systems have been developed (8–11). Cocultures have been especially useful in understanding the interactions between epithelial cells and stromal fibroblasts during normal development and neoplastic transformation. These studies have shown that stromal fibroblasts are essential regulators of normal epithelial cell phenotypes and the malignant phenotypes of preneoplastic or neoplastic epithelial cells (4,5,11).

Epithelial–fibroblast cocultures lend themselves readily to quantitative assessments of the unique differentiated characteristics of either cell type. However, it is less straightforward to quantify the proliferation of only one

The content of this publication does not necessarily reflect the views of the Department of Health and Human Services, nor does mention of trade names, commercial products, or organizations imply endorsement by the U.S. Government.

Contract grant sponsor: DOD Breast Cancer Research Program; Contract grant numbers: DAMD 17-98-1-8063, DAMD 17-00-1-0306, and DAMD 17-00-1-0227; Contract grant sponsor: California Breast Cancer Research Program; Contract grant number: 8KB-0100; Contract grant sponsor: National Institute on Aging; Contract grant number: AG09909; Contract grant sponsor: National Cancer Institute; Contract grant number: NO1-CO-56000; Contract grant sponsor: DOE; Contract grant number: DE-AC03-76SF00098.

*Correspondence to: Judith Campisi, Life Sciences Division, Lawrence Berkeley National Laboratory, 1 Cyclotron Road, MS 84-171, Berkeley, CA 94720.

E-mail: jcampisi@lbl.gov

Published online in Wiley InterScience (www.interscience.wiley.com).
DOI: 10.1002/cyto.10149

cell type in the coculture. This is especially true when the cells are cultured together for extended periods, or when one or both cell types are not easily modified to express a distinguishing marker (e.g., green fluorescent protein, or GFP). Even if cells are marked with GFP, they are typically quantified by fluorescent-activated cell sorting or western blotting, methods that do not permit the assessment of cells in situ. To circumvent these problems, in situ imaging methods have been developed (12–15), but most are not easily applied to different cell types or the experimental conditions described in this study.

We recently reported that senescent human fibroblasts can stimulate hyperproliferation and tumorigenic transformation of premalignant epithelial cells (16). To study the effects of senescent fibroblasts on epithelial cells, we developed a method to quantify epithelial cells that are cocultured with fibroblasts. This method is based on analysis of fluorescent digital images of the cocultures in situ. We describe this method in detail.

MATERIALS AND METHODS

Cells and Cell Culture

Human fibroblast strain WI-38 (ATTC, Rockville, MD), cultured in Dulbecco's modified Eagle's medium (Gibco/BRL, Grand Island, NY) supplemented with 10% fetal bovine serum and passaged at 70–80% confluence underwent replicative senescence after ~50 doublings as described (16,17). Presenescent and senescent cultures contained more than 70% and fewer than 10% proliferating cells, respectively, when subconfluent cells in optimal medium were analyzed for ability to traverse the cell cycle, as described previously (16,17). The presenescent fraction was determined from the percentage of nuclei radiolabeled with [^{3}H]-thymidine during 3 days of exponential growth (labeling index). Premalignant HaCAT (human keratinocytes, from A. Paller, Northwestern University, Chicago, IL) and SCp2 (murine mammary epithelial cells, from P. Desprez, California Pacific Medical Center, San Francisco, CA) epithelial cells were cultured as described elsewhere (16,18,19).

Coculture

Proliferating fibroblasts were trypsinized, suspended in fresh medium, and counted by electronic particle (Coulter) counting. Fibroblasts (5×10^4 presenescent or 1×10^5 senescent) were seeded in six-well culture dishes, allowed to attach overnight, washed extensively, and incubated in serum-free medium for 1–3 days. This protocol arrested the growth of presenescent cells and generated lawns containing similar numbers of presenescent and senescent fibroblasts, as determined by a Coulter counter or hemacytometer. Cell number varied by less than 30%, whether cells were serum starved for 1 or 3 days. Epithelial cells were preincubated in growth factor–deficient medium, described below, for 2–3 days, trypsinized, harvested in trypsin-neutralizing solution (Clonetics, San Diego, CA), counted, and plated (2×10^4/well) onto fibroblast lawns in 2 ml of growth factor–deficient medium. Cocultures were maintained in growth factor–deficient medium for 8 days, unless noted otherwise. Approximately one-half the medium volume was removed and replaced with the fresh medium on day 3 or 4 of coculture to replenish nutrients but not completely deplete growth stimulatory factors produced by the fibroblasts.

Growth factor–deficient medium contained keratinocyte basal medium (KBM, Clonetics), 1.8 mM of $CaCl_2$, 5 μg/ml of insulin, 0.5 μg/ml of hydrocortisone for HaCAT cells and DME/F12 (Gibco/BRL), 5 μg/ml of insulin, 1.4 μM of hydrocortisone, and 5 μg/ml of prolactin for SCp2 cells. Where indicated, the cultures were fixed for 5 min in ice-cold 100% methanol, stained for 5 min with 1 μg/ml of 4,6-diamidino-2-phenylindole (DAPI), washed in phosphate buffered saline (PBS), and viewed and photographed through PBS.

EGFP Expression

Epithelial cells were infected with a retrovirus that expresses enhanced green fluorescent protein (EGFP) and confers neomycin (G418) resistance, as described previously (16), and selected in 300 (SCp2) or 400 (HaCAT) μg/ml of G418 (20). EGFP was expressed at varying levels in more than 90% of the cells, as assessed by fluorescent microscopy and expected for gene expression in mass-infected populations. We counted as positive all cells that exhibited visually detectable fluorescence; cells that did not express GFP had virtually no fluorescence. The GFP expression distribution did not change perceptibly when epithelial cells were seeded onto presenescent or senescent fibroblast lawns.

Image Acquisition

Images were captured from five fields per well at 40× and 200× magnifications with a Nikon inverted fluorescent microscope (Model HB-10101AF), filters suitable for DAPI (blue) or GFP (green) fluorescence, and a Spot CCD camera (Model 1.1.0).

Storage and Software Environment

Images were stored in the Tagged Image File Format for off-line analysis. Custom-made routines (described below) were programmed in C language, compiled, and integrated as a library with the Scil_Image image analysis package (TNO, Amsterdam, The Netherlands). Analyses were carried out on an Ultra 2 Sun workstation (Sun Microsystems, Mountain View, CA) running the Solaris 7 operating system.

Image Analysis

We used a sequence of algorithms to analyze low (40×; Fig. 1) and high (200×; Fig. 2) magnifications of images of DAPI-stained epithelial cells cocultured with fibroblasts. The goal was to quantify the area of each image occupied by the epithelial cells. For high magnification images (Fig. 2), we also estimated the number of epithelial cell nuclei.

We first transformed the original DAPI image (Figs. 1A, 2A) into a gray-scale image by discarding color information (Figs. 1B, 2B) and then automatically corrected shading defects (Figs. 1C, 2C). Shading can be caused by incorrect alignment between the light source and the light

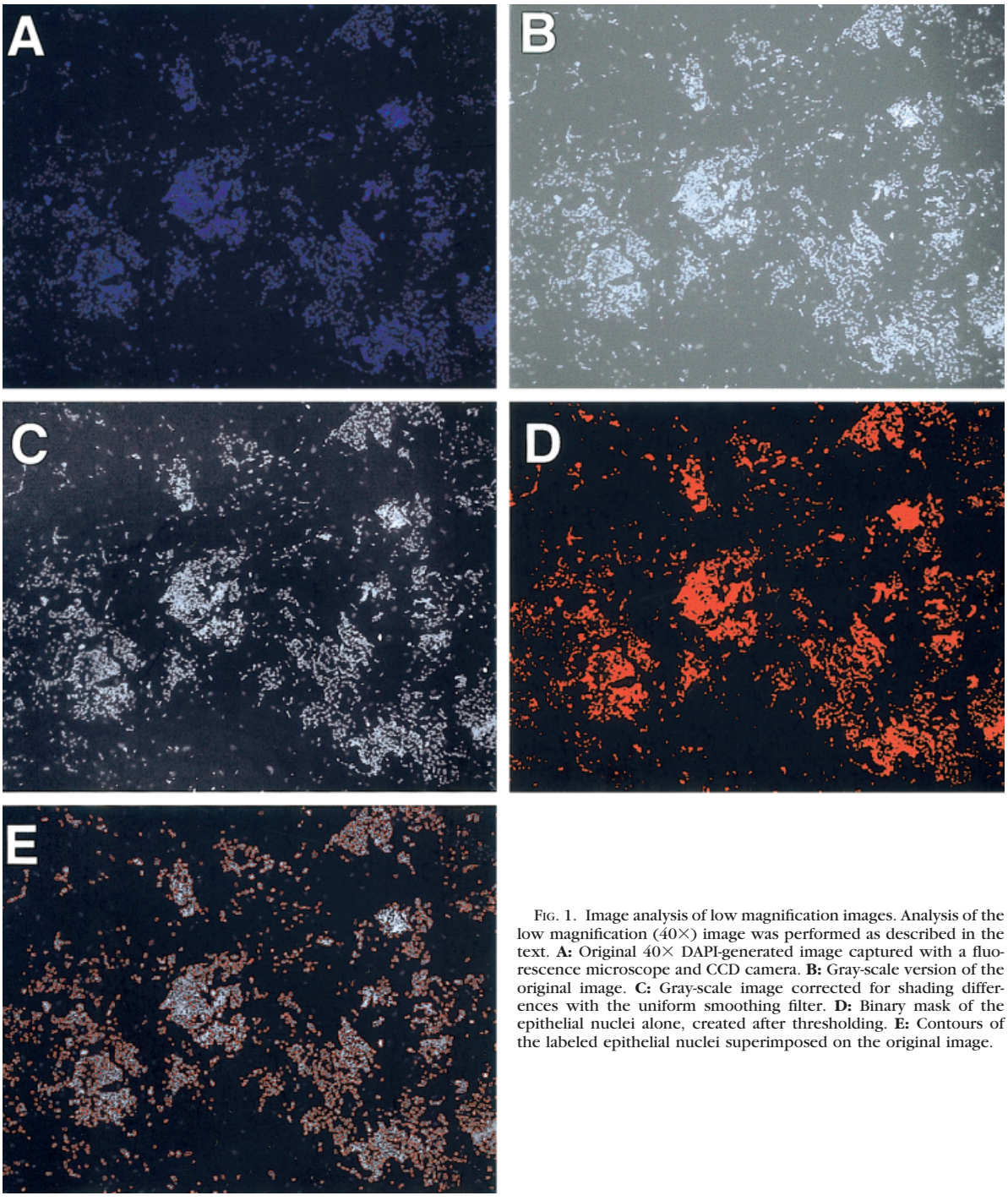

FIG. 1. Image analysis of low magnification images. Analysis of the low magnification (40×) image was performed as described in the text. **A:** Original 40× DAPI-generated image captured with a fluorescence microscope and CCD camera. **B:** Gray-scale version of the original image. **C:** Gray-scale image corrected for shading differences with the uniform smoothing filter. **D:** Binary mask of the epithelial nuclei alone, created after thresholding. **E:** Contours of the labeled epithelial nuclei superimposed on the original image.

path of the microscope or defects in the light bulb, causing gradual, non-uniform illumination of different parts of the field viewed by the microscope and imaged by the camera. Shading correction allows setting the thresholds to identify fibroblasts and epithelial cells based on the difference in their nuclear DAPI intensity. If shading correction was not used, fibroblasts in the bright parts of the image (at the center) would be more intense than epithelial cells in the dimmer parts of the image (at the edges).

To correct for shading differences, the image was spatially filtered with a uniform smoothing filter (kernel size = half the image size). Then, each pixel value in the original image was divided by its intensity in the filtered image and multiplied by the mean pixel intensity of the image. Mathematically, for each pixel:

$$I' = I * \frac{\bar{I}}{U(I)}$$

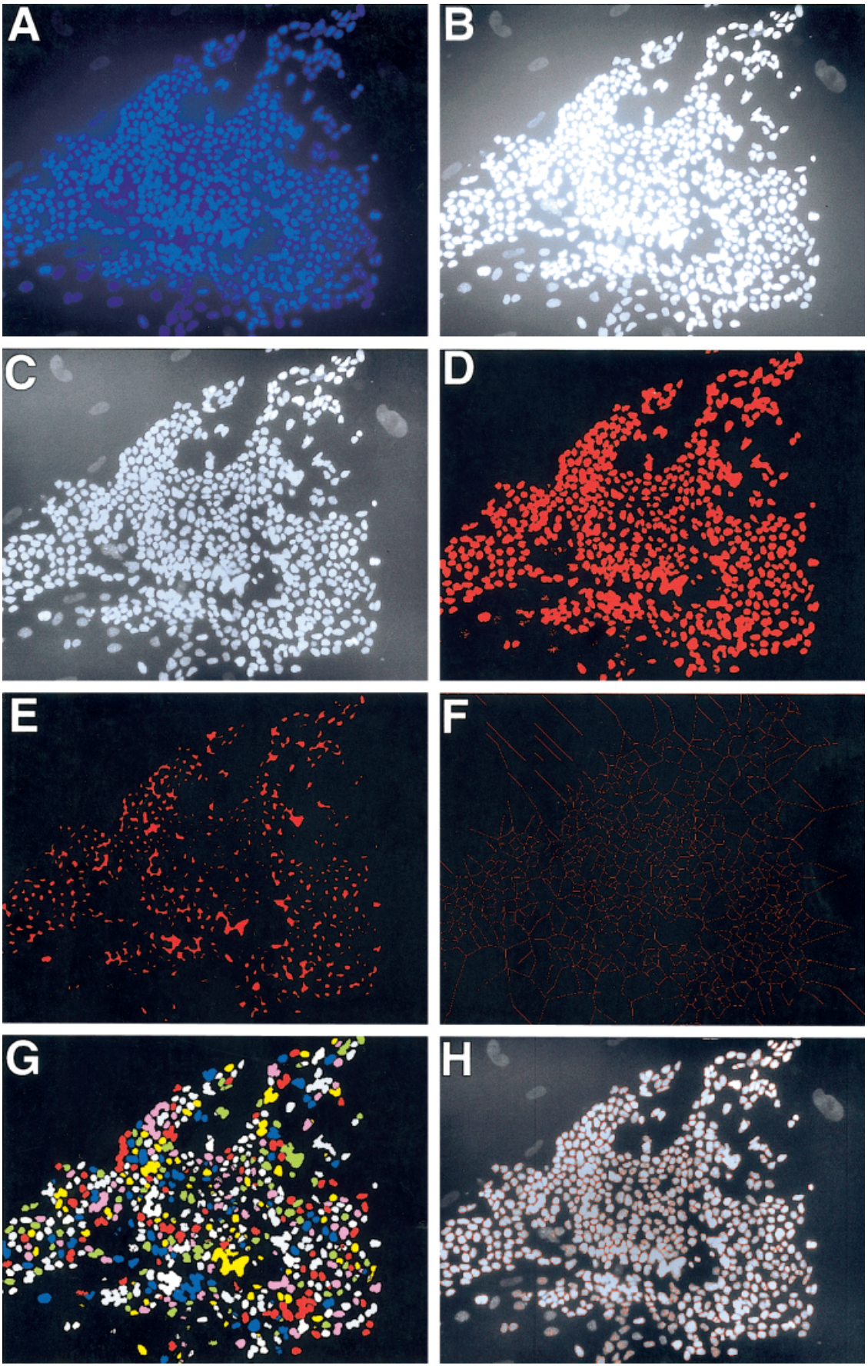

FIG. 2.

where I is the intensity of the pixel in the original image, $\bar{I}$ is the mean pixel intensity of the image, and $U(I)$ is the intensity of the pixel in the filtered image. The kernel size of the filter was considered large enough to produce a flattened background version of the original image. This correction lowers the intensity of areas having a local average intensity higher than the mean, and increases the intensity in areas having a local average intensity lower than the mean.

To ease segmentation of the images by manual thresholding, we contrast-stretched the images by linearly expanding the intensity values of the original range to the maximum allowable image range (0 to 255), thereby increasing the contrast of underexposed images. The images were then manually segmented by using an interactive thresholding tool provided by Scil_Image. This tool allows the user to define a lower (th_l) and a higher (th_h) threshold, thus producing a binary output image (I_{bin}). Pixel intensities in the binary image were 1 where the corresponding pixel intensities in the original image were in the range (th_l–th_h) and 0 elsewhere. The lower threshold was chosen to be higher than the maximum intensity value of the fluorescent emission of the fibroblast nuclei but lower than the emission of the epithelial nuclei. This threshold created a binary mask of epithelial nuclei alone (Figs. 1D, 2D). The binary areas were mostly isolated nuclei, although some contained several nuclei. The total area occupied by epithelial cells was estimated as the number of pixels of value 1 in the binary image.

High magnification images were processed further to divide nuclei clusters into single nuclei and thus obtain better estimates of relative epithelial cell number. We applied a morphologic binary separation filter to the binary image I_{bin}. This filter used a parameter (which we termed "size") related to the average size of nuclei. To obtain the size value, the distance transform (DT) (21) of the binary image was computed, which produced a new image, I_{DT}, where each pixel intensity equaled the distance from the pixel in the binary image to the closest object boundary (DT was computed only for object pixels, not for the background areas). Then, the average value of I_{DT} was calculated by using only pixels within objects and used as the value of size.

To divide clusters of nuclei, I_{DT} was segmented with a threshold value equal to the size, thereby creating a new binary image, I_{sb}, consisting of shrunk versions of all the objects (Fig. 2E). This shrinking step separated clusters into individual shrunk nuclei. Nuclei were then restored to original size as follows. Borders equidistant between shrunk nuclei were automatically identified as the morphologic skeleton of the inverse of the binary image of the shrunk nuclei, I_{SK} (Fig. 2F). Next, the skeleton lines were superimposed on the original image, I_{bin}, to segment the clusters. The binary image of divided nuclei was then labeled, giving a consecutive number to each nonconnected binary object. This way, all pixels belonging to the same object were given the same value, which differed from that given to all other objects. Incomplete objects touching the edges of the image and small objects empirically defined as having an area smaller than three times the squared value of the size were removed. The result was a labeled image (I_{lab}) containing only intact individual nuclei and clusters that were too tightly packed to be divided by the morphologic filter (Fig. 2G).

The contours of the labeled objects were superimposed on the original image for visual inspection and interactive correction (Fig. 2H). At this point, the user could separate undivided clusters by interactively drawing a line between clustered cells with the computer mouse. After detecting erroneously divided nuclei and debris mistaken as nuclei, the user could join the nuclei and remove debris. Although this program still requires considerable operator effort, it is significantly less laborious than manual counting.

The number of nuclei per image was calculated as follows. Segmentation up to this point resulted in a number of objects, a large proportion of which comprised individual nuclei. Objects corresponding to individual nuclei were similar in size, but a few objects were smaller (debris), and some objects were larger, corresponding to clusters of nuclei. An object area histogram was calculated, where each object area was approximated by its number of pixels. Because individual nuclei of similar size comprise most of the image, they populate a few neighboring histogram bins with a large numbers of objects. Larger objects (clusters) fall into bins corresponding to large sizes, but, because their sizes are more variable, they are spread out across more bins. Thus, the histogram has a peak, which is the modal value that represents the average size of individual nuclei. The number of nuclei was calculated as the ratio between the sum of the areas of all objects in the image divided by the average nuclear area. For high magnification images, the output was the number of nuclei (after thresholding to detect only epithelial nuclei) plus the total area occupied by these nuclei, calculated as the sum of the areas of all individual and clustered nuclei. This number was used to estimate the number of epithelial cells per field.

FIG. 2. Image analysis of high magnification images. Analysis of the high magnification (200×) image was performed as described in the text. **A:** Original 200× DAPI-generated image captured with a fluorescence microscope and CCD camera. **B:** Gray-scale version of the original image. **C:** Gray-scale image corrected for shading differences with the uniform smoothing filter. **D:** Binary mask of the epithelial nuclei alone, created after thresholding. **E:** Shrunk version of the objects (epithelial nuclei) in the image. **F:** Morphologic skeleton created by inversion of the binary image shown in E. **G:** Labeled image after applying the morphologic filter. Each nucleus is individually colored. **H:** Contours of the labeled epithelial nuclei superimposed on the original image.

RESULTS

Quantification of DAPI-Stained Cocultures Using High- and Low-Threshold Values

We cocultured premalignant mouse mammary epithelial cells (SCp2) with WI-38 normal human fibroblasts, as described in Materials and Methods. Alternatively, we cultured fibroblasts alone under similar conditions. The cultures were fixed and stained with DAPI, and images of the fluorescent nuclei were captured and stored as described

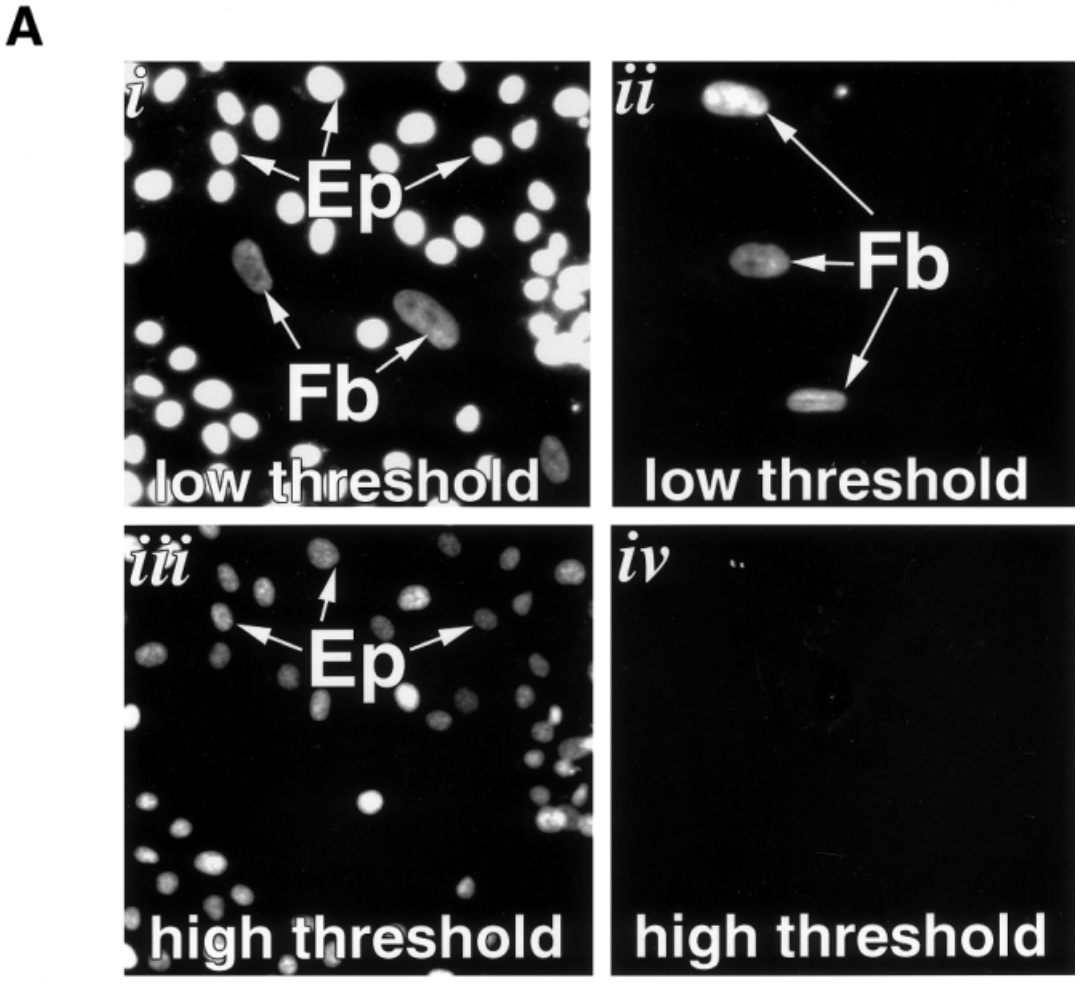
A
i
Ep
Fb
low threshold
ii
Fb
low threshold
iii
Ep
high threshold
iv
high threshold
B
low threshold
high threshold
DAPI Fluorescence
4
3
2
1
0
Ep+Fb
Fb

FIG. 3.

in Materials and Methods. Figure 3A shows an area from a stained epithelial–fibroblast coculture (Fig. 3A, panels *i* and *iii*) and a similar area from a pure fibroblast culture (Fig. 3A, panels *ii* and *iv*). Note that the fibroblast nuclei are generally larger and less intensely stained than the epithelial cell nuclei. When the image threshold was set at a low value, epithelial (Ep) and fibroblast (Fb) nuclei were detectable (Fig. 3A, panels *i* and *ii*). When the image threshold was set at a high value, only the smaller, more intensely stained epithelial nuclei were detected (Fig. 3A, panels *iii* and *iv*). Thus, fibroblast nuclei disappeared from view when a high threshold was used.

We quantified the area of DAPI fluorescence per image that each culture generated when low or high thresholds were applied (Fig. 3B). At a low threshold, epithelial and fibroblast nuclei were detected, and the fluorescent area was proportional to the total number of cells in each culture. The total DAPI fluorescence was always higher in cocultures (Ep + Fb) than in pure fibroblast cultures (Fb) because the cocultures always contained more cells. At a high threshold, pure fibroblasts generated negligible fluorescence, whereas the coculture generated ample fluorescence owing to the presence of the epithelial cells.

The fraction of epithelial cells in the cocultures was proportional to the image area with DAPI fluorescence detected at a high threshold. The fraction of fibroblasts in the cocultures could be estimated by subtracting the area of DAPI fluorescence detected at a high threshold (gray bar, Ep + Fb) from that detected at a low threshold (white bar, Ep + Fb). Moreover, as described in Materials and Methods, the high magnification images could be used to estimate the number of cells per field. The calculated numbers were 27 cells in the fibroblast-only field and 35 fibroblasts and 128 epithelial cells in the coculture field. These numbers compared favorably with those obtained by manual counting: 28 nuclei in the fibroblast-only field and 35 large weakly stained (fibroblast) and 130 small strongly stained (epithelial) nuclei in the coculture field. The calculated numbers were compared with manual counts for five independently analyzed high magnification images, and differences between the two values was never more than 10%.

The high threshold that allowed selective detection of epithelial nuclei was used to quantify epithelial cells in cocultures in all subsequent experiments that used DAPI staining.

FIG. 3. Detection and quantification of fibroblast and epithelial nuclei using high and low threshold values. **A:** Area from a DAPI-stained epithelial–fibroblast coculture (*i* and *iii*) or culture of fibroblasts alone (*ii* and *iv*). The image was analyzed by using a threshold set at a low value, which enables epithelial (Ep) and fibroblast (Fb) nuclei to be seen (*i* and *ii*). The same image was then analyzed by using a high threshold value, which allows only epithelial nuclei to be seen (*iii* and *iv*). Notice the disappearance of fibroblast nuclei when using a high threshold value. **B:** Quantification of the image area with nuclear DAPI fluorescence was performed by using the algorithms described in the text. The results are shown in arbitrary units and are the average value obtained from triplicate wells of epithelial–fibroblast cocultures (left bars, Ep + Fb) or cultures of fibroblasts alone (right bars, Fb). Error bars show the standard error of the means of triplicate wells. White bars, DAPI fluorescence measured by using a low threshold; gray bars, DAPI fluorescence measured by using a high threshold.

DAPI and GFP Quantification of the Same Experiment

To verify that the epithelial DAPI signal is proportional to epithelial cell number, we expressed EGFP in SCp2 and HaCAT (premalignant human keratinocytes) cells. Because we expressed this protein only in the epithelial cells, the area of green fluorescence was directly and exclusively proportional to the number of epithelial cells. We cocultured the EGFP-expressing epithelial cells with WI-38 fibroblasts and compared the area of fluorescence generated by EGFP with that generated by DAPI at a high threshold.

Figure 4 compares the areas covered by DAPI-stained (DAPI) and EGFP-expressing (GFP) SCp2 (Fig. 4A) and HaCAT (Fig. 4B) cells. The cells were cultured alone (C, control) or cocultured with presenescent or senescent fibroblasts. As reported previously (16), fibroblasts stimulated the growth of epithelial cells, and senescent fibroblasts stimulated growth to a greater extent than did presenescent fibroblasts. There was a 20% greater presenescent to senescent fluorescence ratio when GFP was used to quantify epithelial growth, indicating that the number of epithelial cells in presenescent cultures is slightly underestimated by DAPI staining. This underestimation may be due to the smaller difference in DAPI fluorescence between epithelial and presenescent fibroblast nuclei compared with senescent fibroblast nuclei. This variability was acceptable because the growth differences we observed were greater than 200% (i.e., 10 times the error).

For the DAPI values shown in Figure 4A, we verified the number of epithelial nuclei by manually counting each image. Manual counts of five images yielded 4,522 and 13,653 epithelial cells in the presenescent and senescent groups, respectively, giving a senescent to presenescent group ratio of 3.02. These values are in close agreement with the 3.2 ratio obtained by our Scil_Image analysis (1,804 and 5,772 values of epithelial DAPI fluorescence for presenescent and senescent groups, respectively). Thus, image analysis can be used to obtain the relative number of epithelial cells in the presence of fibroblasts and was much less tedious and time consuming than manual counting. We also attempted to use flow cytometry to measure the number of GFP-expressing epithelial cells but found it difficult to obtain single-cell suspensions from epithelial cells grown in coculture (probably due to strong cell–cell interactions), and the resulting cell clumps made quantification unreliable.

Kinetic Studies Using EGFP-Expressing Cells

Although DAPI staining provided a quick, storable method to quantify epithelial cells cocultured with fibroblasts, epithelial cells can be labeled with EGFP (or other vital fluorescent labels), offering the possibility of kinetic studies using the same culture for multiple time points. We show two such studies analyzed by the modified program. First, EGFP-expressing SCp2 cells were seeded onto presenescent or senescent fibroblast lawns (Fig. 5A).

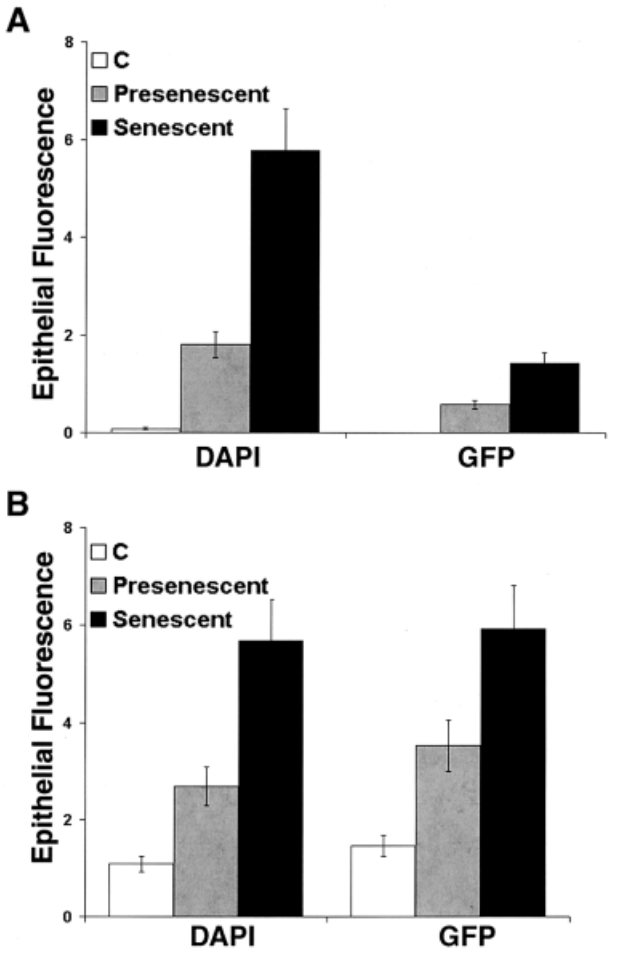

FIG. 4. Comparison of DAPI and EGFP quantification. **A:** EGFP-expressing SCp2 cells were cultured alone (C, white bars) or with presenescent (gray bars) or senescent (black bars) WI-38 fibroblasts. The cultures were stained with DAPI, and image areas of epithelial DAPI fluorescence (detected using a high threshold; left bars) and EGFP fluorescence (right bars) were quantified with the same culture. **B:** EGFP-expressing HaCAT cells were cultured alone (C, white bars) or with presenescent (gray bars) or senescent (black bars) WI-38 fibroblasts. Image areas with DAPI (left bars) and EGFP (right bars) fluorescences were quantified as described in A. The results are shown in arbitrary units and are the average value obtained from triplicate wells. Error bars show the standard error of the means of triplicate wells.

After the indicated number of days, the cocultures were removed from the incubator, photographed, and returned to the incubator. Second, we used two chamber dishes (Millicell, Millipore Corp., Bedford, MA) in which upper and lower wells are separated by a membrane that permits diffusible molecules, but not cells, to pass. EGFP-expressing HaCAT cells were seeded in the upper wells, and lower wells contained either no cells (C) or presenescent or senescent fibroblasts (Fig. 5B), and the cultures were photographed on successive days. Analysis of the images showed that presenescent and senescent fibroblasts stimulate exponential epithelial cell growth. However, senescent fibroblasts stimulated faster growth, especially during the first 4 days of culture. In addition, at least some of the stimulation caused by fibroblasts was due to diffusible factors that they produce. Thus, the program can be used for kinetic studies of cells stained with a vital fluorescent marker.

To determine whether the ratios obtained by image analysis corresponded to the total number of epithelial cells, we counted (using an inverted fluorescent microscope) the number of GFP-positive cells per dish on day 5 of coculture, at which time the number of epithelial cells per dish was within an acceptable range for manual counting. We counted 6,008 epithelial cells per well in the presenescent group and 26,153 in senescent group, for a senescent to presenescent group ratio of 4.35. Analysis of five GFP fluorescence image areas produced values of 38,311 and 9,005 for the senescent and presenescent groups, respectively, or a ratio of

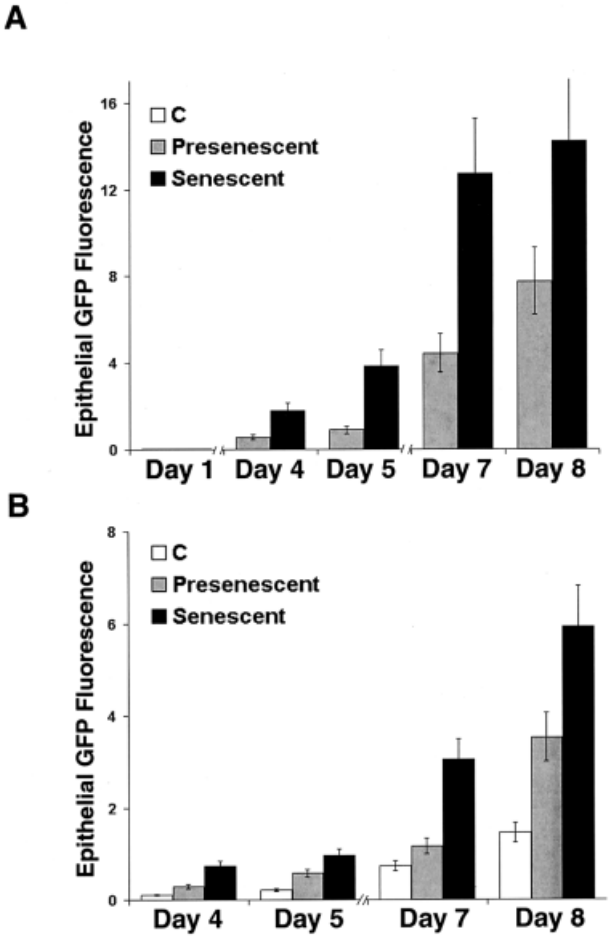

FIG. 5. Kinetic studies. **A:** EGFP-labeled SCp2 cells were grown in coculture with presenescent or senescent fibroblasts as described in Materials and Methods. After the indicated number of days, the cocultures were removed from the incubator, photographed, and returned to the incubator. The images were used for quantification. Error bars are the standard error of the means of duplicate wells. Gray bars, presenescent lawns; black bars, senescent lawns. **B:** EGFP-expressing HaCAT cells were seeded into the upper wells of two-chamber culture dishes. The lower well contained medium alone or presenescent or senescent fibroblast lawns. The same cultures were photographed on multiple days after seeding, and the images were used for quantification. Error bars are the standard error of the means of duplicate wells. White bars, epithelial cells alone; gray bars, presenescent lawns; black bars, senescent lawns.

4.25. Thus, manual counting and the image analysis program provided very similar ratios. We estimated that, on average, image analysis is two to three times faster than manual counting.

One can also use epithelial DAPI or EGFP fluorescence to detect and normalize for possible differences in the ability of epithelial cells to attach to culture dishes or fibroblast lawns. For this purpose, images can be captured immediately after attachment of the epithelial cells, and the fluorescence signals can be used to normalize fluorescent signals from all subsequent time points. In this way, it is possible to distinguish between poor attachment and lack of cell growth. We observed no significant differences in the ability of epithelial cells to attach to presenescent or senescent fibroblasts in the cocultures quantified in Figure 5A (not shown).

DISCUSSION

We have reported a useful image analysis–based method for quantifying a large number of fluorescently labeled cells. The method is reliable, accurate, visually verifiable, and interactively correctable. We specifically developed this method to monitor epithelial cell proliferation in the presence of fibroblasts. The method overcomes some common problems associated with monitoring the proliferation of one cell type in the presence of other cells. Labeled cells (EGFP-expressing or immunolabeled for a specific marker) can, of course, be manually counted under the microscope. However, manual counting is time consuming and laborious. Flow cytometry also can be used to quantify labeled cells in a mixed population. Common problems associated with this method include cell clumping, when cells with strong cell–cell interactions (as with most epithelial cells) are analyzed, which confounds the results, and the requirement for fairly large sample sizes.

We evaluated our method with two different means to identify cells: expression of EGFP in the cells whose growth was monitored and staining epithelial–fibroblast cocultures with the DNA intercalating dye DAPI. In comparing the growth of epithelial cells under various culture conditions, both identification methods yielded similar results (<20% difference) and compared favorably with manual counting.

EGFP labeling was particularly versatile because it enabled kinetic studies of cell growth. Thus, the same culture of cells labeled with a vital fluorescence marker could be followed for multiple time points. This is a unique feature of our method. We expect it can be used to follow a variety of biological processes, including cell proliferation, chemotaxis, and invasiveness. DAPI staining allowed for quantification of unmodified cells. This approach enables samples to be fixed and stored for analysis at a later time. However, it requires that there be a large enough difference in nuclear staining intensity between the cell type whose behavior is monitored and that of the other cells in the culture—the smaller the difference, the more inaccurate the quantification.

Our image analysis method can be extended to quantify any cell type in a mixed cell population, provided that cell type can be uniquely identified by a fluorescent marker. Examples include, but are not limited to, cells stained for a particular protein by immunofluorescence. For example, cells expressing differentiation-specific proteins can be quantified in heterogeneous cultures, or only cells expressing this protein above a certain threshold level can be quantified, facilitating the use of immunofluorescence microscopy as a quantitative tool.

ACKNOWLEDGMENTS

This work was supported by a postdoctoral fellowship from the DOD Breast Cancer Research Program (DAMD17-98-1-8063 to A.K.), research grants from the California Breast Cancer Research Program (8KB-0100 to A.K.), the National Institute on Aging (AG09909 to J.C.), DOD (DAMD17-00-1-0306 and DAMD17-00-1-0227 to C.O.S.), the National Cancer Institute (NO1-CO-56000 to S.L.), and a DOE contract (DE-AC03-76SF00098) to the University of California.

LITERATURE CITED

1. Chidgey AP, Boyd RL. Thymic stromal cells and positive selection. APMIS 2001;109:481–492.
2. Cunha GR, Hom YK. Role of mesenchymal-epithelial interactions in mammary gland development. J Mammary Gland Biol Neoplasia 1996; 1:21–35.
3. Sariola H, Sainio K. Cell lineages in the embryonic kidney: their inductive interactions and signaling molecules. Biochem Cell Biol 1998;76:1009–1016.
4. Elenbaas B, Weinberg RA. Heterotypic signaling between epithelial tumor cells and fibroblasts in carcinoma formation. Exp Cell Res 2001;264:169–184.
5. Silberstein GB. Tumour-stromal interactions. Role of the stroma in mammary development. Breast Cancer Res 2001;3:218–223.
6. Chrenek MA, Wong P, Weaver VM. Tumour-stromal interactions. Integrins and cell adhesions as modulators of mammary cell survival and transformation. Breast Cancer Res 2001;3:224–229.
7. Schmeichel KL, Weaver VM, Bissell MJ. Structural cues from the tissue microenvironment are essential determinants of the human mammary epithelial cell phenotype. J Mammary Gland Biol Neoplasia 1997;3: 201–113.
8. Nishikawa M, Tahara T, Hinohara A, Miyajima A, Nakahata T, Shimosaka A. Role of the microenvironment of the embryonic aorta-gonad-mesonephros region in hematopoiesis. Ann NY Acad Sci 2001;938: 109–116.
9. Berthier-Vergnes O, Gaucherand M, Peguet-Navarro J, Plouet J, Pageaux JF, Schmitt D, Staquet MJ. Human melanoma cells inhibit the earliest differentiation steps of human Langerhans cell precursors but failed to affect the functional maturation of epidermal Langerhans cells. Br J Cancer 2001;85:1944–1951.
10. Habib FK, Ross M, Bayne CW. Development of a new in vitro model for the study of benign prostatic hyperplasia. Prostate 2000;9(suppl): 15–20.
11. Olumi AF, Grossfeld GD, Hayward SW, Carroll PR, Tlsty TD, Cunha GR. Carcinoma-associated fibroblasts direct tumor progression of initiated human prostatic epithelium. Cancer Res 1999;59:5002–5011.
12. Chassoux D, Franchi J, Cao TT, Debey P. DNA content by in situ fluorescence imaging and S-phase detection, with chromatin structure preserved. Anal Quant Cytol Histol 1999;21:489–497.
13. Mehes G, Lorch T, Ambros PF. Quantitative analysis of disseminated tumor cells in the bone marrow by automated fluorescence image analysis. Cytometry 2000;42:357.
14. Windhagen A, Maniak S, Heidenreich F. Analysis of cerebrospinal fluid cells by flow cytometry and immunocytochemistry in inflammatory central nervous system diseases: comparison of low- and high-density cell surface antigen expression. Diagn Cytopathol 1999;21: 313–318.
15. Lockett SJ, O'Rand M, Rinehart C, Kaufman D, Herman B, Jacobson K. Automated fluorescence image cytometry: DNA quantification and

detection of chlamydiae infections. Anal Quant Cytol Histol 1991;13: 27.
16. Krtolica A, Parrinello S, Lockett S, Desprez P-Y, Campisi J. Senescent fibroblasts promote epithelial cell growth and tumorigenesis: a link between cancer and aging. Proc Natl Acad Sci USA 2001;98:12072–12077.
17. Dimri GP, Lee X, Basile G, Acosta M, Scott G, Roskelley C, Medrano EE, Linskens M, Rubelj I, Pereira-Smith O, Peacocke M, Campisi J. A biomarker that identifies senescent human cells in culture and in aging skin in vivo. Proc Natl Acad Sci USA 1995;92:9363–9367.
18. Skobe M, Fusenig NE. Tumorigenic conversion of immortal human keratinocytes through stromal cell activation. Proc Natl Acad Sci USA 1998;95:1050–1055.
19. Desprez P-Y, Roskelley C, Campisi J, Bissell MJ. Isolation of functional cell lines from a mouse mammary epithelial cell strain: the importance of basement membrane and cell-cell interactions. Mol Cell Differen 1993;1:99–110.
20. Dimri GP, Itahana K, Acosta M, Campisi J. Regulation of a senescence checkpoint response by the E2F1 transcription factor and p14(ARF) tumor suppressor. Mol Cell Biol 2000;20:273–285.
21. Castleman KR. Digital image processing. Englewood Cliffs, NJ: Prentice-Hall; 1996. p 475–477.